INSTITUT DE FRANCE
Académie des sciences

Comptes Rendus

Chimie

Habiba Guédouar, Hanane Zaki, Mohammed Bouachrine
and Faouzi Aloui

Molecular docking investigation of cytotoxic phenanthrene derivatives

Volume 23, issue 4-5 (2020), p. 329-342

Published online: 10 November 2020

https://doi.org/10.5802/crchim.27

Les Comptes Rendus. Chimie *sont membres du*
Centre Mersenne pour l'édition scientifique ouverte
www.centre-mersenne.org
e-ISSN : 1878-1543

Comptes Rendus
Chimie
2020, 23, nº 4-5, p. 329-342
https://doi.org/10.5802/crchim.27

Preliminary communication / *Communication*

Molecular docking investigation of cytotoxic phenanthrene derivatives

Etude de l'amarrage moléculaire de dérivés phénanthréniques cytotoxiques

Habiba Guédouar[a], Hanane Zaki[b], Mohammed Bouachrine*[b, c] and Faouzi Aloui*[a]

[a] University of Monastir, Faculty of Sciences, Laboratory of Asymmetric Synthesis and Molecular Engineering of Materials for Organic Electronics (LR18ES19), Avenue of Environment, 5019 Monastir, Tunisia

[b] Molecular and Computational Chemistry, Molecular Chemistry and Natural Substances Laboratory, Faculty of Sciences, University Moulay Ismail of Meknes, BP 11201 Zitoune, Meknes, Morocco

[c] EST Khenifra, Sultan Moulay Slimane University, Khenifra, BP 170, 54000 Khenifra, Morocco

E-mails: habiba.gued@gmail.com (H. Guédouar), mmezakihanane@gmail.com (H. Zaki), bouachrine@gmail.com (M. Bouachrine), aloui.faouzi@laposte.net (F. Aloui)

Abstract. Our previous experimental work indicated that the presence of ester functionality in phenanthrene derivatives **D-1** and **D-2** leads to potent cytotoxicity against the *Caco-2* cell line. The present work is based on th-is experimental result. First, we optimized the structures of the studied molecules using the density functional theory method. Then we performed a study about their potential biological importance by evaluating the binding mode and exploring their intermolecular interactions with appropriate proteins using molecular docking calculations. Consequently, we confirmed the results obtained from experimental studies. In particular, our study indicated that many promising proteins are able to bind and interact with the phenanthrene skeleton from the binding site. Methyl 8-methyl-9,10-phenanthrenequinone-3-carboxylate **D-1** and methyl 8-methyldibenzo[*a,c*]phenazine-3-carboxylate **D-2** displayed strong cytotoxicity. However, the best affinity is noted for B-Raf proto-oncogene serine/threonine-protein kinase (-9.8 Kcal/mol for molecule **D-1** and -11.1 Kcal/mol for molecule **D-2**), which is higher than that of any other protein used. Especially, this protein is involved in sending signals inside cells that are involved in directing cell growth and is found to be a significant target in both types of studied cancers.

Résumé. Nos travaux expérimentaux antérieurs ont indiqué que la présence de la fonction ester sur les dérivés phénanthréniques **D-1** et **D-2** a montré une cytotoxicité puissante contre la lignée cellulaire *Caco-2*. Dans ce présent travail, nous nous basons sur ces résultats obtenus expérimentalement. Tout d'abord, nous avons optimisé à l'aide de la méthode DFT les structures des molécules étudiées, puis

* Corresponding authors.

nous avons mené l'étude de leur importance biologique en évaluant le mode de liaison et en explorant leurs interactions intermoléculaires avec des protéines appropriées à l'aide des calculs d'amarrage moléculaire. Par conséquent, nous avons confirmé les résultats obtenus suite aux études expérimentales. En particulier, notre étude a indiqué que de nombreuses protéines prometteuses sont capables de se lier et d'interagir avec le squelette phénanthrénique à partir du site de liaison. Le 8-méthyl-9,10-phénanthrénequinone-3-carboxylate de méthyle **D-1** et le 8-méthyldibenzo[*a,c*]phénazine-3-carboxylate de méthyle **D-2** ont montré une forte cytotoxicité. La meilleure affinité est observée avec la protéine B-Raf proto-oncogène sérine/thréonine kinase (-9.8 Kcal/mol pour la molécule **D-1** et -11.1 Kcal/mol pour la molécule **D-2**) qui est plus importante que celle de toute autre protéine utilisée. Ajoutons que, cette protéine est impliquée dans l'envoi de signaux à l'intérieur des cellules qui participent à la direction de la croissance cellulaire et se révèle être une cible significative dans les deux types de cancers étudiés.

Keywords. Phenanthrene, Cytotoxicity, DFT calculations, Molecular modeling, Docking, Proteins.

Manuscript received 27th February 2020, revised 7th April 2020, accepted 14th April 2020.

1. Introduction

Polycyclic compounds based on aromatic hydrocarbons are considered attractive targets for synthesizing medicinal units since they exhibit favorable properties such as stability and ease of synthesis and possess high biological responses, particularly anticancer activity [1]. As a result, many researchers around the world have become interested in the preparation and development of new cytotoxic molecules [2–4]. In this context, H. Guédouar and co-workers [2] worked on the synthesis of a fairly large number of new phenanthrene skeletons, using a simple procedure, with the aim of preparing promising active compounds for the development of anticancer agents. In fact, they prepared a variety of tricyclic compounds by modifying the central structure of phenanthrene. The compounds were evaluated for their *in vitro* cytotoxic activity against two tumor cell lines. Interestingly, the analysis of the IC_{50} values suggests that most compounds exert cytotoxic effects with selectivity. Among them, methyl 8-methyl-9,10-phenanthrenequinone-3-carboxylate **D-1** (IC_{50} = 0.97 μg/mL) and methyl 8-methyldibenzo[*a,c*]phenazine-3-carboxylate **D-2** (IC_{50} = 1.09 μg/mL) are interesting substrates due to their highest potency against the *Caco-2* cancer cell (Figure 1).

In this study, molecular docking was performed on the two most active *O*-linked molecules **D-1** and **D-2**, previously prepared by H. Guédouar and co-workers to identify the key structural features required to design new potent candidates of this class. Thus, the results extracted from this study might be useful to design potent antitumor drugs. Before performing the molecular docking, the studied molecules were optimized using the density functional theory (DFT) method. In recent years, the DFT has become the most popular quantum chemical method for computing several molecular properties such as those exhibited by chemical, physical, and biological systems [5–7]. The reported quantum chemical calculations were performed at the B3LYP/6-31G(d,p) level of theory [8–10]. The geometry optimization in the gas phases was carried out using the Gaussian 09 suite of programs [11].

2. Molecular docking study

Molecular docking analysis is a reliable method for the evaluation of binding affinity and the prediction of intermolecular interactions of novel compounds containing potential receptors [12,13]. We performed molecular docking studies for eight vital cancer targets (Table 1). Our research was based on the crystal structures of receptors with bound ligand molecules. This structure was obtained from X-ray crystal data of RCSB Protein Data Bank (PDB) [14–16].

In the majority of selected structures, co-crystallized ligand molecules are known drugs with proven action. Thus they were utilized to predict the binding site location [17] as well as to serve as references in our analysis. As previously demonstrated [2], molecules **D-1** and **D-2**, whose 3D-QSAR structures are shown in Figure 2, are the most active. Docking studies of both compounds were carried out to analyze their ability to interact with each target for which the binding site locations are shown in Table 2.

Each enzyme does not necessarily contain a single active site. We chose the active site of interest

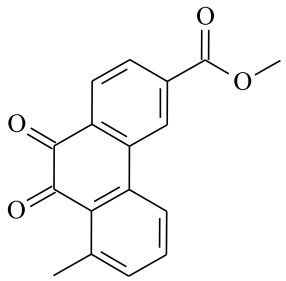

D-1

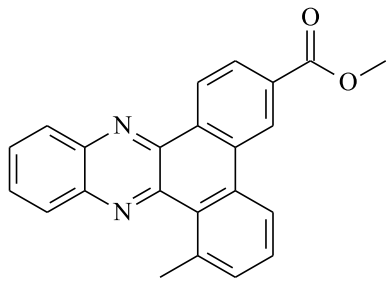

D-2

Figure 1. Chemical structures of the studied phenanthrenes **D-1** and **D-2**.

Table 1. Protein database used for docking study and their native ligands

PDB code	Name	Native ligand	Chain
2HYY	Human Proto-oncogene tyrosine-protein kinase ABL1	Imatinib	A
3C4C	B-Raf proto-oncogene serine/threonine-protein kinase	PLX4720	A
3EWH	Vascular endothelial growth factor receptor 2	Pyridyl-pyrimidine benzimidazole	A
3RCD	Receptor tyrosine-protein kinase erbB-2	TAK-285	A
3W2S	Epidermal growth factor receptor	W2R	A
4JT5	Serine/threonine-protein kinase mTOR	Torkinib (PP242)	A
4U5J	Proto-oncogene tyrosine-protein kinase Src	Ruxolitinib	A
6N2J	GTPase KRas	Tetrahydropyridopyrimidines	A

Table 2. Binding site location for each target

PDB code	X	Y	Z
2HYY	14.251	15.282	17.632
3C4C	0.478	−2.111	−19.745
3EWH	15.131	−5.231	10.046
3RCD	13.047	1.810	28.168
3W2S	5.726	0.748	12.742
4JT5	51.856	−0.015	−49.145
4U5J	−8.382	26.909	5.045
6N2J	22.52	2.591	−22.481

to the study, which contains the reference inhibitor (which is the drug site); (X, Y and Z) are the three-dimensional coordinates of the active site of interest (in this case, inhibition of the enzyme).

2.1. *Docking results*

With the aim of confirming the potential cytotoxicity of our phenanthrene derivatives **D-1** and **D-2**, we evaluated the binding mode and explored their intermolecular interactions with appropriate proteins. The docking results are summarized in Table 3. The binding affinity was evaluated by the binding free energy (Kcal/mol). In fact, all the studied targets can establish binding with the two studied ligands. The tricyclic compound **D-1** exhibited binding energies ranging from −9.8 to −8.3 kcal/mol. The molecular docking study with molecule **D-2** revealed a binding energy ranging from −11.1 to −9.2 kcal/mol. This slight difference in energy is probably due to the size of the studied molecules. Indeed, molecule **D-1** is tricyclic while **D-2** is composed of five cycles, one of which is heterocyclic.

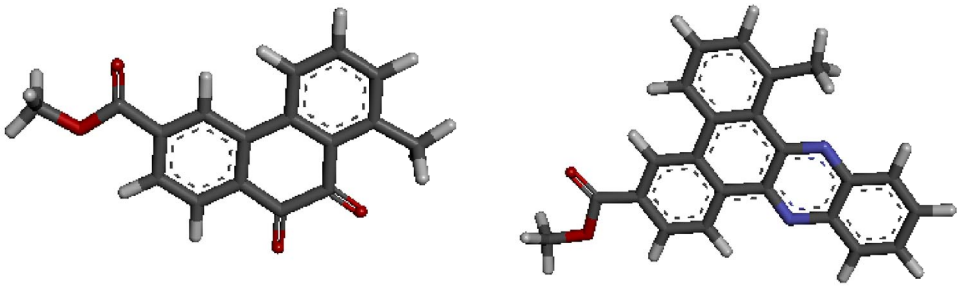

Figure 2. 3D-QSAR structures of compounds **D-1** (a) and **D-2** (b) used for the docking study.

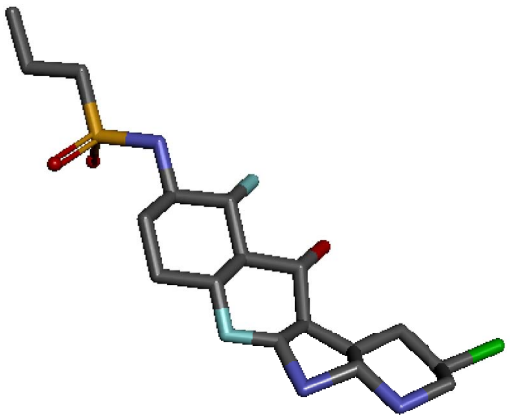

Figure 3. 3D structure of the native ligand **PLX4720**.

Table 3. Docking score expressed in kcal/mol

PDB code	Molecule **D-1**	Molecule **D-2**
2HYY	−8.3	−9.2
3C4C	−9.8	−11.1
3EWH	−9.4	−10.1
3RCD	−9.2	−10.3
3W2S	−9.0	−10.1
4JT5	−8.9	−10.2
4U5J	−9.4	−10.4
6N2J	−9.0	−9.4

In addition, the data shown in Table 3 indicate that both molecules show a very high affinity to and stability with all the studied targets. In particular, the highest affinity is noted for the protein B-Raf proto-oncogene serine/threonine-protein kinase (PDB code 3C4C) [18,19]. In fact, the affinity between molecule **D-1** and 3C4C is found to be about −9.8 Kcal/mol. The affinity between 3C4C and molecule **D-2** is about −11.1 Kcal/mol. We can conclude from these results that the B-Raf protein is the most likely target for this molecule. Thus, it is worth noting that this protein is involved in sending signals inside cells that are involved in directing cell growth. It regulates cell proliferation and growth, cell survival, cell mobility, protein biosynthesis, and transcription, which suggests that it is the most targeted protein by our tricyclic molecule.

Moreover, it is believed that the remarkable activity of molecules **D-1** and **D-2** is related to their stability, which is explained by the numbers and types of bonds established with the studied potential targets. These descriptors are mentioned in Table 4, and the details of the interactions are presented in Table 5. In this regard, the amino acids VAL 471, PHE 583, LYS 483, ALA 481, and TRP 531 are found to be important for the antiproliferative activity of our molecules since they form bonds in both cases. As expected for 3C4C, it appears that the hydrogen bond formed with the amino acid ASP 594 increases affinity to the target, which in turn increases the activity of both molecules.

The positioning of each molecule in the active site and the binding pocket are shown in Table 6.

Based on affinity, stability, and the study of different interactions, we can ensure that B-Raf proto-oncogene serine/threonine-protein kinase is the

Table 4. Modes and types of bonds between the studied molecules and their potential target

PDB code	D-1	D-2
2HYY	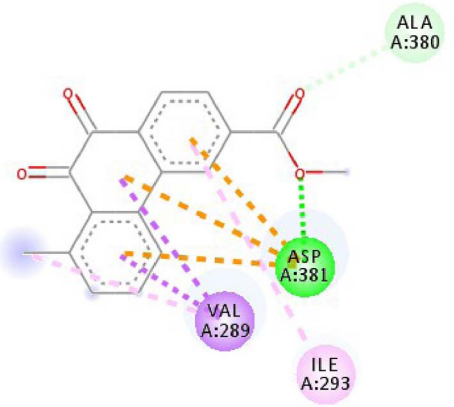	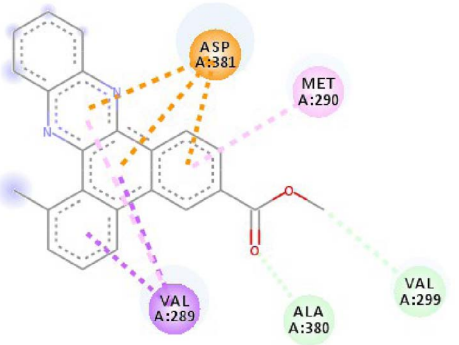
3C4C	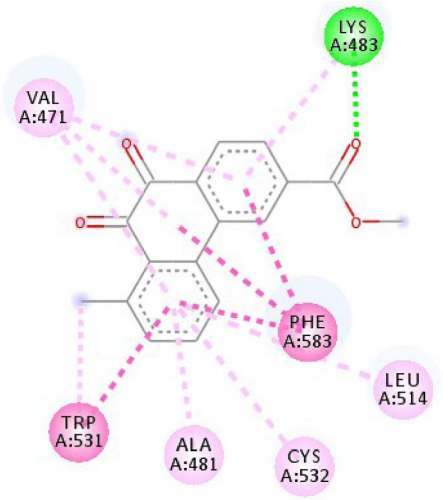	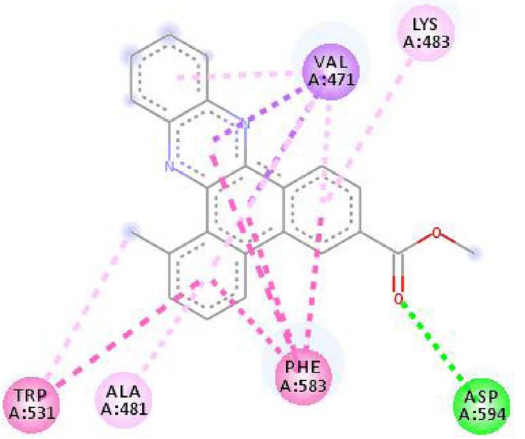
3EWH	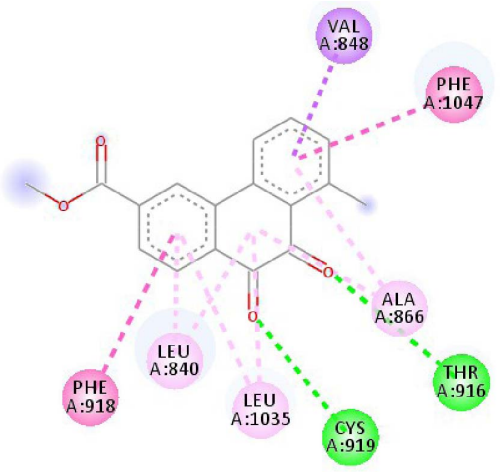	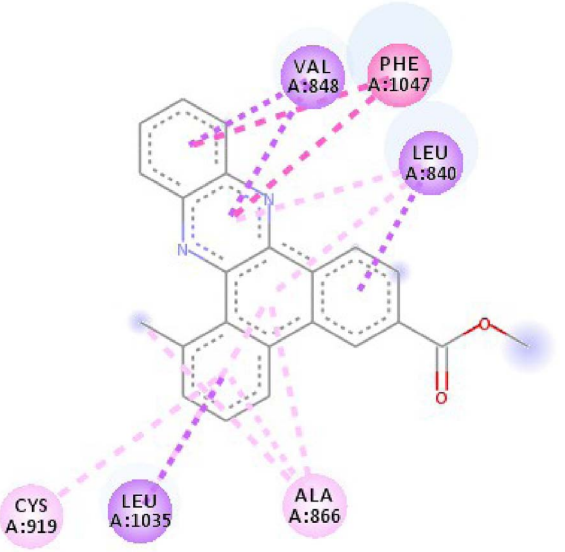

(continued on next page)

Table 4. (continued)

PDB code	D-1	D-2
3RCD	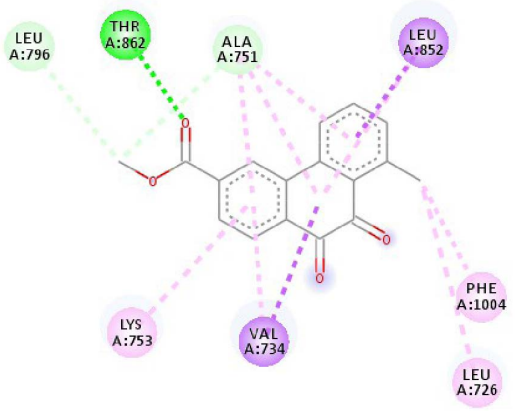	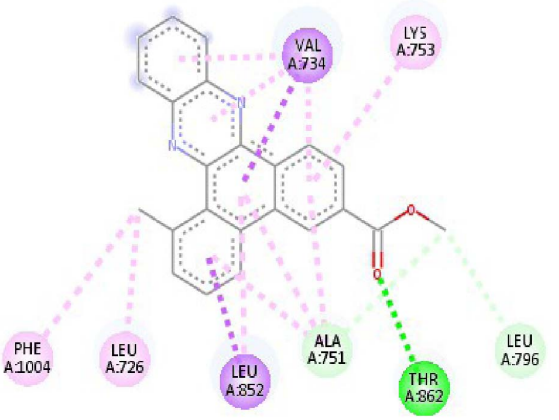
3W2S	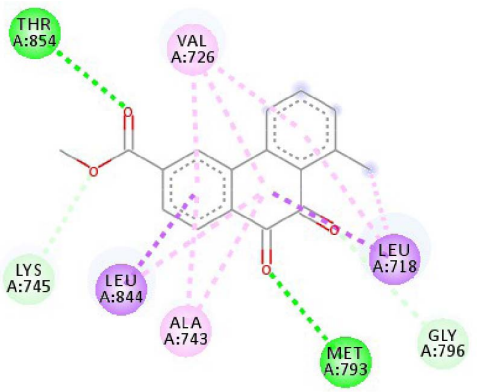	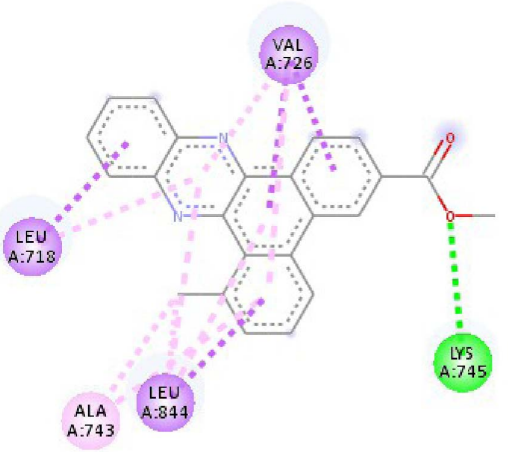
4JT5	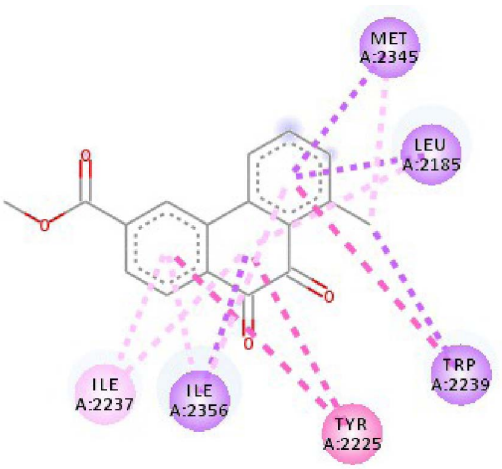	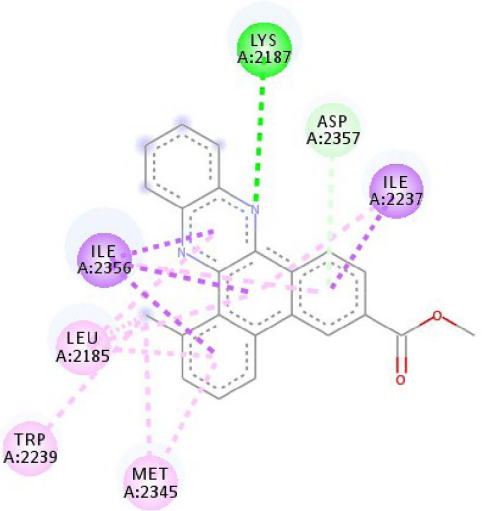

(continued on next page)

Table 4. (continued)

PDB code	D-1	D-2
4U5J	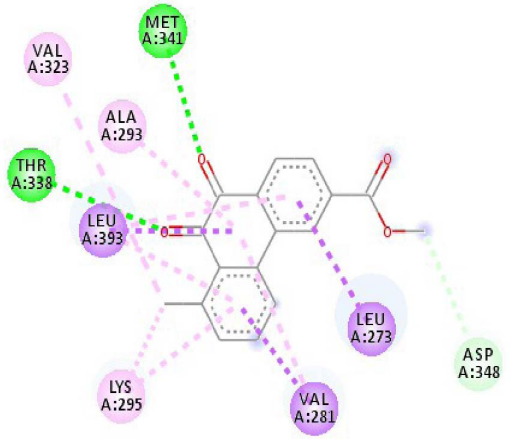	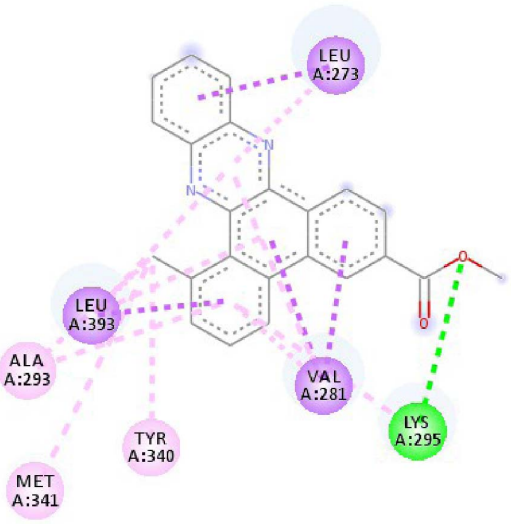
6N2J	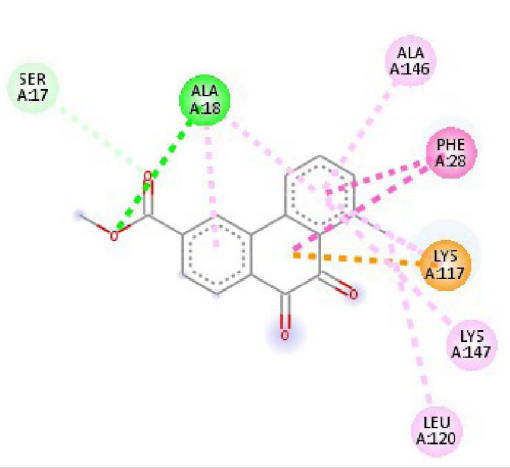	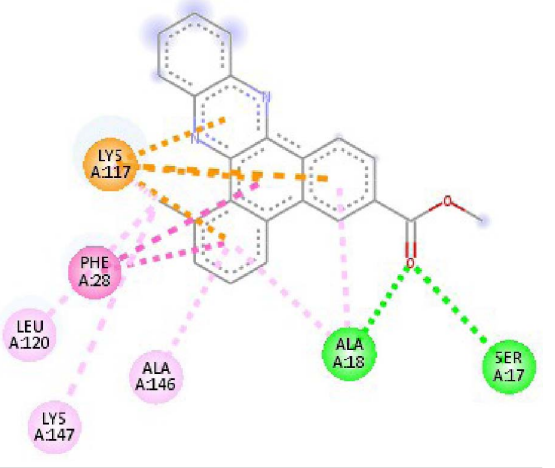

Interactions

- Conventional Hydrogen Bond
- π-Anion, π-Cation
- Carbon Hydrogen Bond
- π-Donor Hydrogen Bond
- π-σ
- π- π T-shaped
- Alkyl
- π-Alkyl

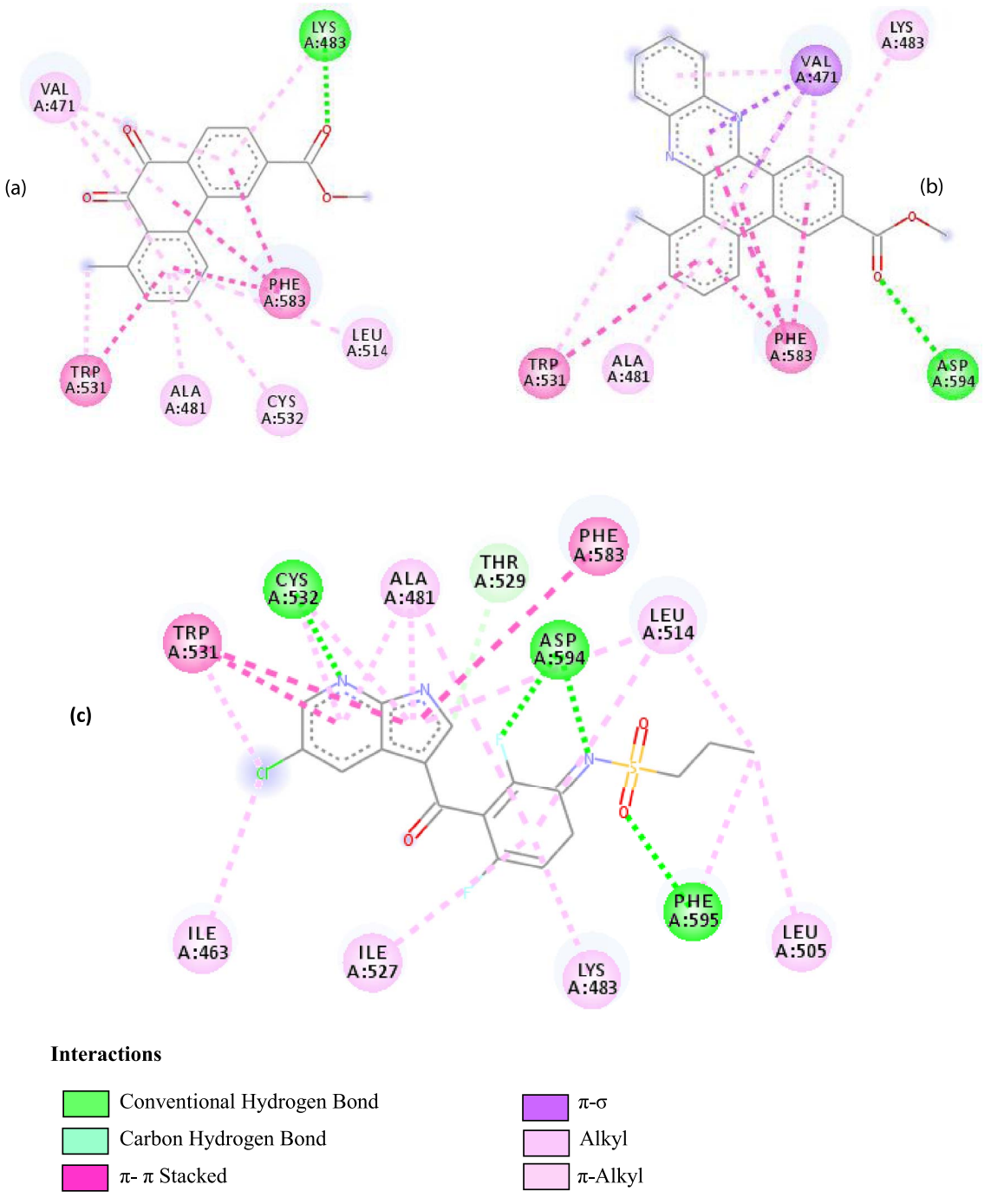

Figure 4. Interactions between the protein B-Raf proto-oncogene serine/threonine-protein kinase and molecule **D-1** (a), molecule **D-2** (b), and the native ligand **PLX4720** (c).

Table 5. Details of the different interactions

Target	D-1	D-2	Target	D-1	D-2
2HYY	ASP 381 NH–O ligand	ALA 380 C–O ligand	**3W2S**	MET 793 NH–O ligand	LYS 745 NH–O ligand
	ALA 330 C–O ligand	VAL 299 O–C ligand		THR 854 OH–O ligand	LEU 718 C–π ligand
	ASP 381 O–π ligand	ASP 381 O–π ligand		LYS 745 C–O ligand	VAL 726 C–π ligand
	ASP 381 O–π ligand	ASP 381 O–π ligand		GLY 796 C–O ligand	VAL 726 C–π ligand
	ASP 381 O–π ligand	ASP 381 O–π ligand		LEU 718 C–π ligand	LEU 844 C–π ligand
	VAL 289 C–π ligand	VAL 289 C–π ligand		LEU 844 C–π ligand	ALA 743 π–C ligand
	VAL 289 π–C ligand	VAL 289 C–π ligand		LEU 718 π–C ligand	LEU 844 π–C ligand
	ILE 293 π–π ligand	MET 290 π–π ligand		VAL 726 π–π ligand	LEU 844 π–π ligand
		VAL 289 π–π ligand		ALA 743 π–π ligand	LEU 718 π–π ligand
				VAL 726 π–π ligand	VAL 726 π–π ligand
				ALA 743 π–π ligand	LEU 844 π–π ligand
				LEU 844 π–π ligand	VAL 726 π–π ligand
				VAL 726 π–π ligand	ALA 743 π–π ligand
3C4C	LYS 483 NH–O ligand	ASP 594 NH–O ligand	**4JT5**	LEU 2185 C–π ligand	LYS 2187 NH–N ligand
	TRP 531 π–π ligand	VAL 471 C–π ligand		MET 2345 C–π ligand	ASP 2357 N–π ligand
	PHE 583 π–π ligand	VAL 471 C–π ligand		ILE 2356 C–π ligand	ILE 2237 C–π ligand
	PHE 583 π–π ligand	TRP 531 π–π ligand		TRP 2239 π–π ligand	ILE 2356 C–π ligand
	PHE 583 π–π ligand	PHE 583 π–π ligand		TYR 2225 π–π ligand	ILE 2356 C–π ligand
	TRP 531 π–C ligand	PHE 583 π–π ligand		TYR 2225 π–π ligand	ILE 2356 C–π ligand
	VAL 471 π–π ligand	PHE 583 π–π ligand		MET 2345 π–C ligand	ILE 2356 C–π ligand
	LYS 483 π–π ligand	PHE 583 π–π ligand		ILE 2237 π–π ligand	LEU 2195 π–C ligand
	VAL 471 π–π ligand	TRP 531 π–C ligand		ILE 2356 π–π ligand	MET 2345 π–C ligand
	VAL 471 π–π ligand	VAL 471 π–π ligand		LEU 2285 π–π ligand	TRP 2239 π–C ligand
	ALA 481 π–π ligand	VAL 471 π–π ligand		ILE 2237 π–π ligand	ILE 2356 π–π ligand
	LEU 514 π–π ligand	VAL 471 π–π ligand		ILE 2356 π–π ligand	LEU 2185 π–π ligand
	CYS 532 π–π ligand	LYS 483 π–π ligand			ILE 2237 π–π ligand
		ALA 481 π–π ligand			LEU 2185 π–π ligand
		CYS 532 π–π ligand			LEU 2185 π–π ligand
					MET 2345 π–π ligand
3EWH	THR 916 OH–O ligand	LEU 840 C–π ligand	**4U5J**	THR 338 OH–O ligand	LYS 295 NH–O ligand
	CYS 919 NH–O ligand	VAL 848 C–π ligand		MET 341 NH–O ligand	LEU 273 C–π ligand
	VAL 848 C–π ligand	VAL 848 C–π ligand		ASP 348 OH–C ligand	VAL 281 C–π ligand
	PHE 918 π–π ligand	LEU 1035 C–π ligand		LEU 273 C–π ligand	VAL 281 C–π ligand
	PHE 1074 π–π ligand	PHE 1047 π–π ligand		VAL 281 C–π ligand	LEU 393 C–π ligand
	LEU 840 π–π ligand	PHE 1047 π–π ligand		LEU 393 C–π ligand	ALA 293 π–C ligand
	LEU 1035 π–π ligand	ALA 866 π–C ligand		LYS 295 π–C ligand	MET 341 π–C ligand
	LEU 1035 π–π ligand	LEU 840 π–π ligand		VAL 323 π–C ligand	LEU 393 π–C ligand
	LEU 840 π–π ligand	ALA 866 π–π ligand		LEU 393 π–π ligand	TYR 340 C–π ligand

(continued on next page)

Table 5. (continued)

Target	**D-1**	**D-2**	Target	**D-1**	**D-2**
	ALA 866 π–π ligand	LEU 1035 π–π ligand		VAL 281 π–π ligand	LEU 393 π–π ligand
	ALA 866 π–π ligand	LEU 840 π–π ligand		ALA 293 π–π ligand	LEU 273 π–π ligand
		ALA 866 π–π ligand		LYS 295 π–π ligand	VAL 281 π–π ligand
		CYS 919 π–π ligand		LEU 393 π–π ligand	LEU 393 π–π ligand
					VAL 281 π–π ligand
					VAL 293 π–π ligand
					LYS 295 π–π ligand
3RCD	THR 862 OH–O ligand	THR 862 OH–O ligand	**6N2J**	ALA 18 NH–O ligand	SER17 N–O ligand
	ALA 751 OH–C ligand	ALA 571 O–C ligand		SER 17 C–O ligand	ALA 18 N–O ligand
	LEU 796 O–C ligand	LEU 796 O–C ligand		LYS 117 N–π ligand	LYS 117 N–π ligand
	VAL 734 C–π ligand	VAL 734 C–π ligand		PHE 28 π–π ligand	LYS 117 N–π ligand
	LEU 852 C–π ligand	LEU 852 C–π ligand		PHE 28 π–π ligand	LYS 117 N–π ligand
	LEU 726 π–C ligand	LEU 726 π–C ligand		LYS 117 π–C ligand	LYS 117 N–π ligand
	PHE 1004 π–C ligand	PHE 1004 π–C ligand		LEU 120 π–C ligand	PHE 28 π–π ligand
	VAL 734 π–π ligand	VAL 734 π–π ligand		ALA 18 π–π ligand	PHE 28 π–π ligand
	ALA 751 π–π ligand	ALA 751 π–π ligand		LYS 117 π–π ligand	LYS 117 π–C ligand
	LYS 753 π–π ligand	LYS 753 π–π ligand		ALA 18 π–π ligand	LEU 120 π–C ligand
	ALA 751 π–π ligand	ALA 751 π–π ligand		LYS 117 π–π ligand	LYS 147 π–C ligand
	LEU 852 π–π ligand	LEU 852 π–π ligand		ALA 146 π–π ligand	ALA 18 π–π ligand
	ALA 751 π–π ligand	VAL 734 π–π ligand		LYS 147 π–π ligand	LYS 117 π–π ligand
		ALA 751 π–π ligand			ALA 18 π–π ligand
		VAL 734 π–π ligand			LYS 117 π–π ligand
					ALA 146 π–π ligand

potential target for these molecules. To better confirm these results, we have compared the types and numbers of bonds of our molecules **D-1** and **D-2** with those of the native ligand **PLX4720** (Figure 3).

It can be seen from the comparison of the interactions between the potential target and the studied molecules as well as the reference molecule that most of the amino acids that interact with the reference molecule also interact with our studied molecules. These interactions are essentially hydrophobic bonds, hydrogen bonds, and π-interactions (Figure 4).

3. Conclusion

Following the study of H. Guédouar and co-workers that evaluated the antiproliferative activity of phenanthrene derivatives against the *Caco-2* cancer cell line, this study proposed two molecules that exhibited the best activity against this cancerous cell. For understanding the mode of action of these molecules to propose a potential therapeutic target in the two types of studied cancers, we established molecular docking against eight vital cancer targets. As a result, molecular docking results confirmed that tricyclic molecules **D-1** and **D-2** show significant activity. Both of the studied compounds were found to display low binding energies and the best affinity is noted in the protein B-Raf proto-oncogene serine/threonine-protein kinase, which is an important target in both types of studied cancers. Moreover, the comparison of the types and the modes of interactions between these molecules and the reference ligand, which is an inhibitor of this protein,

Table 6. Positioning and the binding pocket of each molecule in the active site

PDB code	D-1	D-2
2HYY	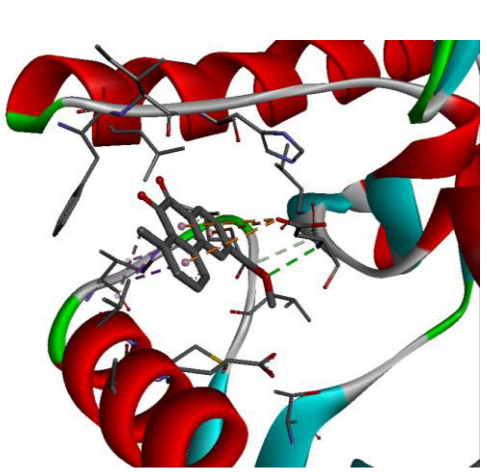	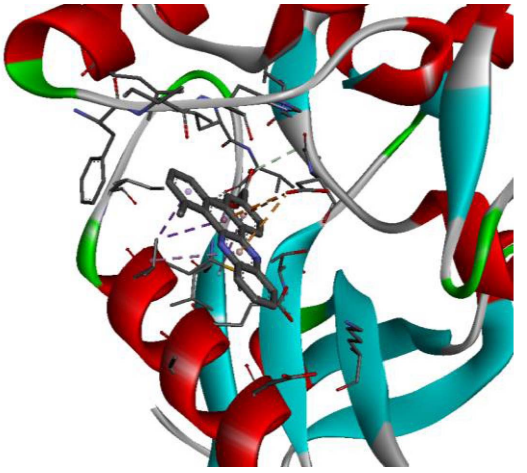
3C4C	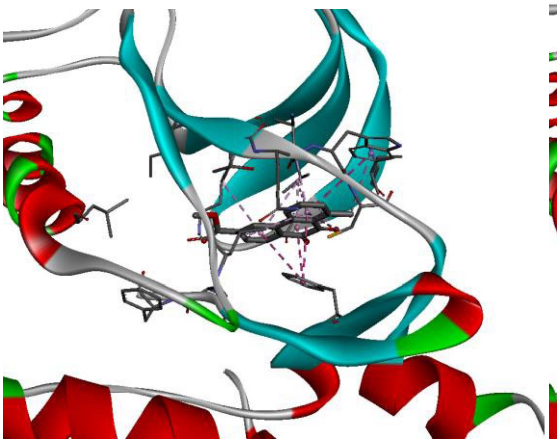	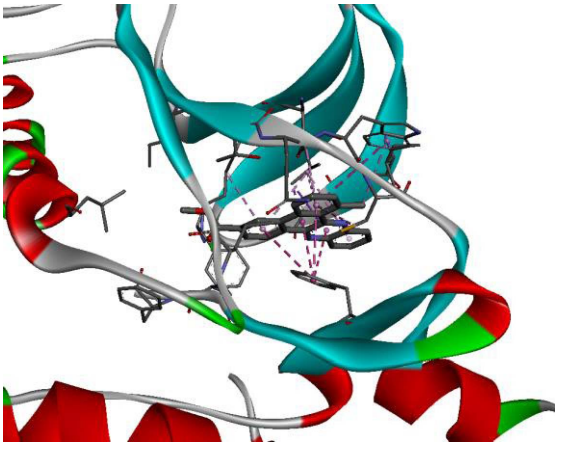
3EWH	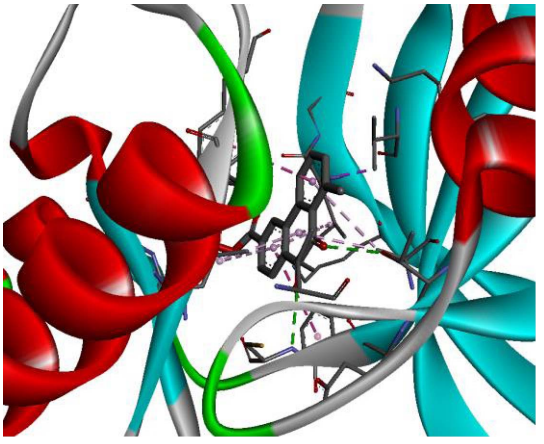	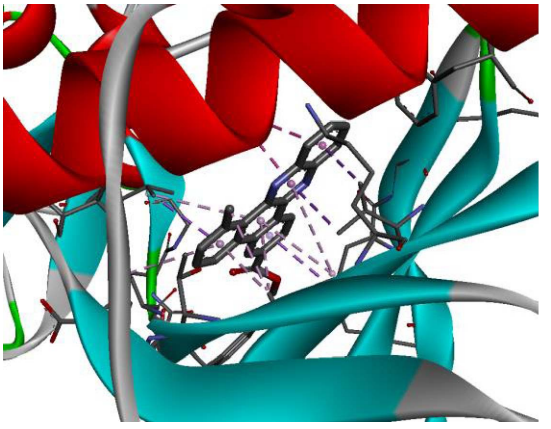

(continued on next page)

Table 6. (continued)

PDB code	D-1	D-2
3RCD	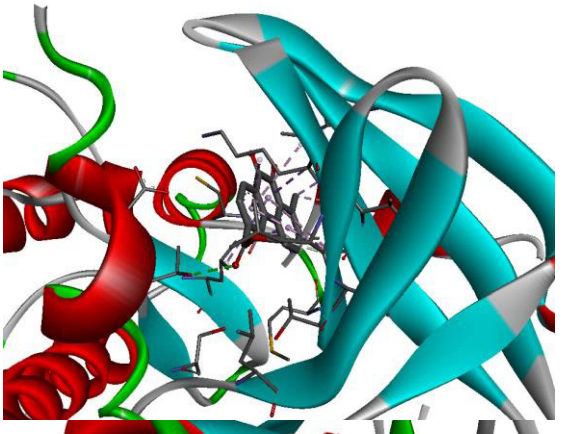	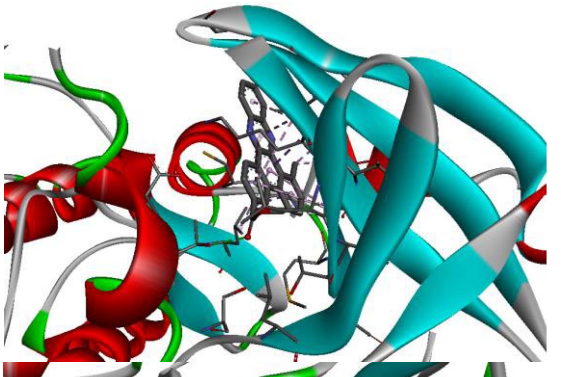
3W2S	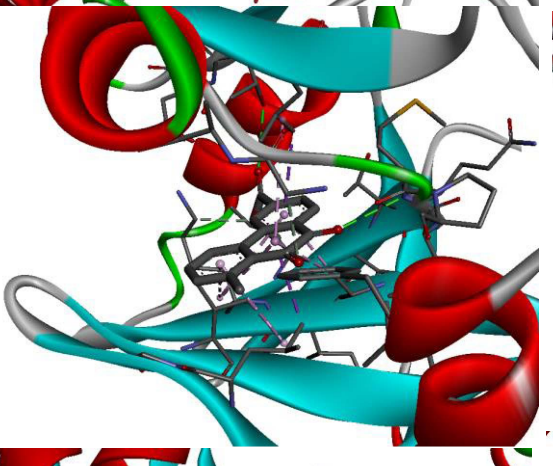	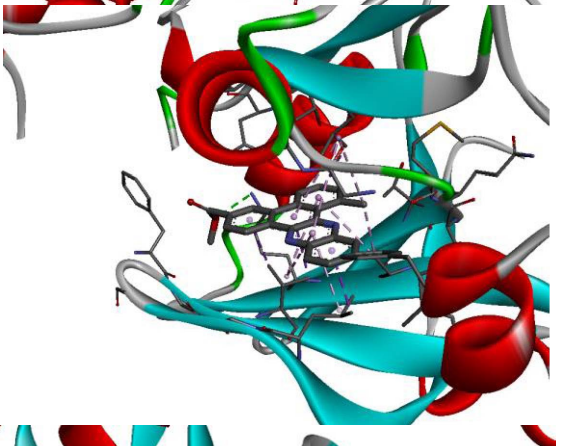
4JT5	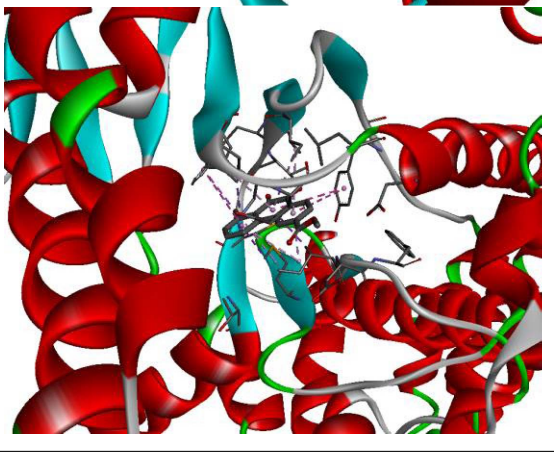	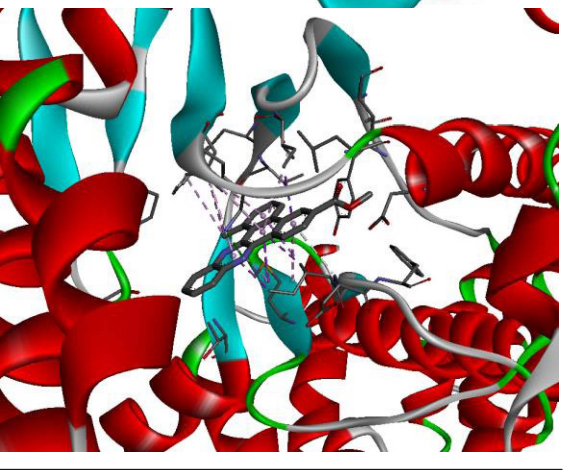

(continued on next page)

shows remarkable similarity in the binding of amino acids in the types of interactions, which suggests that molecules **D-1** and **D-2** are ligands that can inhibit this protein.

Table 6. (continued)

PDB code	D-1	D-2
4U5J	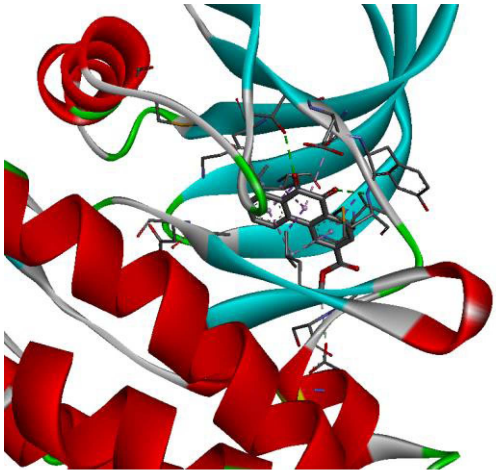	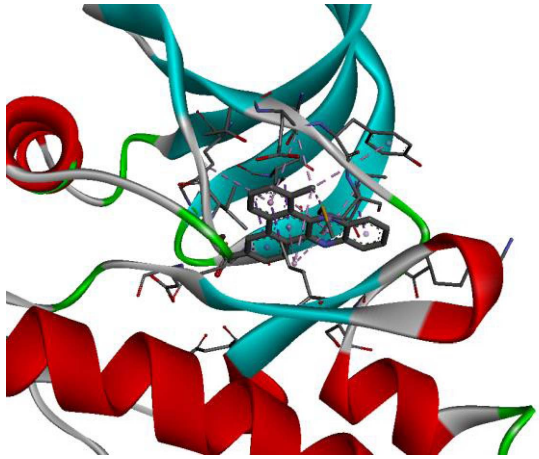
6N2J	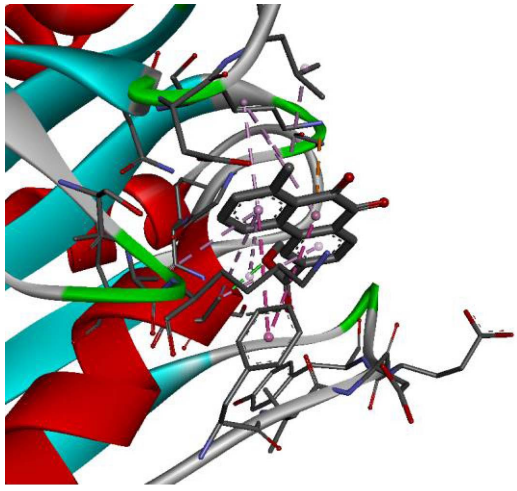	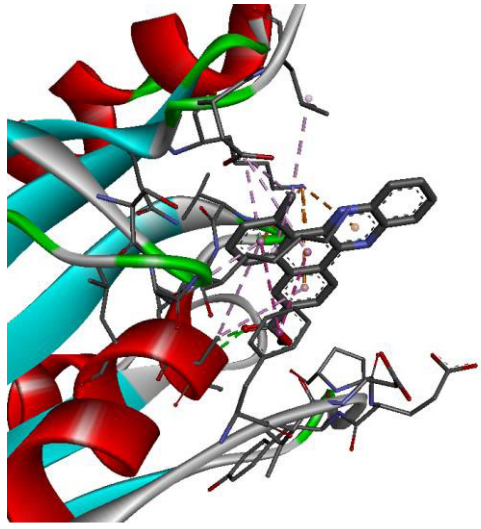

Acknowledgment

The authors are grateful to the Direction Générale de la Recherche Scientifique (DGRS) of the Tunisian Ministry of Higher Education and Scientific Research for financial support.

References

[1] A. Kovacs, A. Vasas, J. Hohmann, *Phytochemistry*, 2008, **69**, 1084-1110.

[2] H. Guédouar, F. Aloui, A. Beltifa, H. Ben Mansour, B. Ben Hassine, *C. R. Chim.*, 2017, **8**, 841-849.

[3] H. Guédouar, F. Aloui, B. Ben Hassine, *J. Adv. Chem.*, 2016, **12**, 4404-4412.

[4] H. Guédouar, B. Ben Hassine, F. Aloui, *C. R. Chim.*, 2019, **22**, 310-315.

[5] S. W. Smith, *The Scientist and Engineer's Guide to Digital Signal Processing*, California Technical Publishing, 1997, 169 pages.

[6] T. V. Mourik, M. Bühl, M. P. Gaigeot, *Phil. Trans. R. Soc. A*, 2011, **2014**, 372-393.

[7] S. Raugei, F. L. Gervasio, P. Carloni, *Phys. Stat. Sol. (b)*, 2006, **243**, 2500-2515.

[8] A. Gümüş, S. Gümüş, *Maced. J. Chem. Chem. Eng.*, 2017, **36**, 239-249.

[9] G. W. Ejuh, F. T. Nya, N. Djongyang, J. M. B. Ndjaka, *Opt. Quantum Electron.*, 2018, **336**, 336-345.

[10] K. P. Vijayalakshmi, C. H. Suresh, *Org. Biomol. Chem.*, 2008, **6**, 4384-4390.
[11] A. Karton, *Chem. Phys. Lett.*, 2014, **614**, 156-161.
[12] A. M. Dar, S. Mir, *Anal. Bioanal. Tech.*, 2017, **8**, 1-3.
[13] R. B. Jacob, T. Andersen, O. M. McDougal, *PLoS Comput. Biol.*, 2012, **8**, 1-5.
[14] C. Zardecki, S. Dutta, D. S. Goodsell, M. Voigt, S. K. Burley, *J. Chem. Educ.*, 2016, **93**, 569-575.
[15] P. W. Rose, A. Prlić, A. Altunkaya, C. Bi, A. R. Bradley, C. H. Christie, L. D. Costanzo, J. M. Duarte, S. Dutta, Z. Feng, R. K. Green, D. S. Goodsell, B. Hudson, T. Kalro, R. Lowe, E. Peisach, C. Randle, A. S. Rose, C. Shao, Y. P. Tao, Y. Valasatava, M. Voigt, J. D. Westbrook, J. Woo, H. Yang, J. Y. Young, C. Zardecki, H. M. Berman, S. K. Burley, *Nucleic Acids Res.*, 2017, **45**, D271-D281.
[16] S. K. Burley, H. M. Berman, C. Bhikadiya, C. Bi, L. Chen, L. D. Costanzo, C. Christie, K. Dalenberg, J. M. Duarte, S. Dutta, Z. Feng, S. Ghosh, D. S. Goodsell, R. K. Green, V. Guranović, D. Guzenko, B. P. Hudson, T. Kalro, Y. Liang, R. Lowe, H. Namkoong, E. Peisach, I. Periskova, A. Prlić, C. Randle, A. Rose, P. Rose, R. Sala, M. Sekharan, C. Shao, L. Tan, Y. P. Tao, Y. Valasatava, M. Voigt, J. Westbrook, J. Woo, H. Yang, J. Young, M. Zhuravleva, C. Zardecki, *Nucleic Acids Res.*, 2019, **47**, D464-D474.
[17] D. J. Matthews, M. E. Gerritsen, *Targeting Protein Kinases for Cancer Therapy*, Wiley, Hoboken, N.J., 2010.
[18] G. Sithanandam, W. Kolch, F. M. Duh, U. R. Rapp, *Oncogene*, 1990, **5**, 1775-1780.
[19] G. Sithanandam, T. Druck, L. A. Cannizzaro, G. Leuzzi, K. Huebner, U. R. Rapp, *Oncogene*, 1992, **7**, 795-799.